

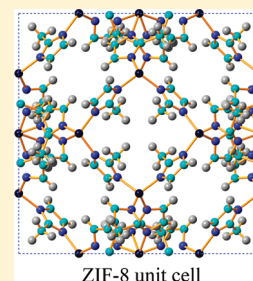
Force Field for Molecular Dynamics Computations in Flexible ZIF-8 Framework

Bin Zheng, Marco Sant,* Pierfranco Demontis, and Giuseppe B. Suffritti

Dipartimento di Chimica, Università di Sassari, Via Vienna 2, Sassari I-07100, Italy

S Supporting Information

ABSTRACT: Correct modeling of framework flexibility plays a major role in obtaining accurate results when performing atomistic simulations of guest molecule diffusion within ZIF crystal structures. Here we present a full set of force field parameters, based on the AMBER database and on previously computed partial charges, well reproducing the ZIF-8 structural properties over a wide range of temperatures and pressures. To test our model, the self-diffusivity for sorbed carbon-dioxide is computed and is found to be in good agreement with experimental measurements. Our results are also compared to the ones obtained with other charge models and are found to be more accurate. Finally, an estimate of the influence on self-diffusion of various simulation details is given.



ZIF-8 unit cell

1. INTRODUCTION

In recent years, intensive research activity related to porous materials has involved the study of tunable pore geometry in order to improve the selectivity and storage properties of sorbents. As a result, metal–organic frameworks (MOFs) with flexible organic linkers and bridging tetrahedral metal ions were extensively investigated. In particular, zeolitic imidazolate frameworks (ZIFs), a subfamily of MOFs, have attracted great attention due to their exceptional chemical and thermal stability, which are very desirable features in zeolitic structures.^{1,2}

Enormous efforts have been made in synthesizing new types of ZIFs and in understanding the mechanisms behind their properties. Investigations showed that some key factors, such as the type of metal atoms and organic linkers, as well as the cage geometry and flexibility, play a major role in the thermodynamics and dynamics of guest molecules.^{3–5} Among others, the effect due to the ZIFs lattice flexibility is very interesting, from both a theoretical and an applicative point of view. On one hand, the structure and properties of the host lattice can change at very high loading; in ZIF-8, for example, this occurs due to the reorientation of the 2-methylimidazole (MeIM) organic linkers.^{6,7} On the other hand, the flexibility of the framework influences the dynamics of the sorbed guest molecules. In this view, IR microscopy, kinetic uptake experiments and chromatographic studies have shown that nitrogen (having kinetic diameter of ~ 3.6 Å), methane (~ 3.8 Å), ethane (~ 3.8 Å), and propane (~ 4.0 Å) can be adsorbed in ZIF-7 and ZIF-8 structures: this would be impossible in a rigid framework since these structures have window opening diameters of ~ 3.0 Å and ~ 3.4 Å, respectively.^{8–11} Besides, huge differences in the diffusion coefficients of guest molecules within rigid or flexible ZIF structures were obtained,⁴ even for small guest molecules.⁵ On this basis, the framework flexibility should be taken into consideration for an accurate study of the dynamics of the molecules sorbed within ZIFs,^{10,12} this is particularly true

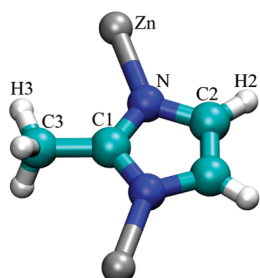
for molecular simulations, which play an important role in complementing the experimental measurements in the investigation and prediction of ZIF's properties, microscopic mechanisms and potential applications.^{10,13–19} Nonetheless, the assumption of rigid framework, with atoms fixed at their crystallographic positions, is still employed in most of current molecular simulations, due to the lack of a suitable force field for modeling flexible frameworks. The complexity in modeling a flexible crystal arises from the treatment of the forces representing chemical bonds (bonded forces).^{20,21} This term, in fact, determines the flexibility of the framework itself and, if not properly chosen, may lead to a lattice collapse or to a completely rigid framework. At the same time, the modeling of the electrostatic interaction, as part of the nonbonded force, is very important since it determines the electronic properties of the framework, such as quadrupolar moment and polarization. The modeling of this term is not trivial, as demonstrated by the existence of various methods for computing the framework charge distribution.²² Because of the complexity of building suitable force fields, until now, only few attempts have been made to model flexible ZIF systems. Hertäg et al.⁴ investigated the diffusion of CH₄ in ZIF-8, but their flexible force field cannot reproduce very accurately the crystal structure, namely bond lengths and bond angles, measured via X-ray diffraction (XRD) experiments.¹ The flexible framework model of Battisti et al.,⁵ instead, matches closely the geometrical parameters of the ZIFs unit cells, but the lack of partial charges lowers the accuracy on the dynamics of polar molecules. To the best of our knowledge, a complete and reliable force field for molecular simulation of a flexible ZIF-8 system has not been developed yet.

Received: September 30, 2011

Revised: November 23, 2011

Published: December 13, 2011

Table 1. Force Field Parameters for ZIF-8 Flexible Framework



bonding potential: $E_{\text{bond}} = K_b(b - b_0)^2$		
bond type	K_b (kcal·mol ⁻¹ ·Å ⁻²)	b_0 (Å)
C1-C3	346.543	1.490
C1-N	488.000	1.335
C2-N	440.210	1.370
C2-H2	367.000	1.080
C2-C2	540.249	1.350
C3-H3	340.000	1.090
Zn-N	78.500	2.011

bending potential: $E_{\text{bend}} = K_\theta(\theta - \theta_0)^2$		
angle type	K_θ (kcal·mol ⁻¹ ·rad ⁻²)	θ_0 (°)
N-C1-N	75.484	112.16
N-C1-C3	66.015	123.92
C2-C2-N	73.750	108.65
C2-C2-H2	49.451	125.67
N-C2-H2	49.954	125.68
C1-C3-H3	48.088	109.32
C1-N-C2	71.254	105.27
C1-N-Zn	48.680	128.33
C2-N-Zn	32.477	126.40
N-Zn-N	35.240	109.48
H3-C3-H3	35.000	109.50

dihedral: $E_{\text{proper}} = K_\phi [1 + \cos(n\phi - \phi_0)]$			
type ^a	K_ϕ (kcal·mol ⁻¹)	n	ϕ_0 (°)
X-N-C2-X	2.325	2	180.0
X-C2-C2-X	5.150	2	180.0
X-C1-N-X	5.000	2	180.0

improper: $E_{\text{improper}} = K_\phi (\phi - \phi_0)^2$		
type ^b	K_ϕ (kcal·mol ⁻¹ ·rad ⁻²)	ϕ_0 (°)
N-C3-C1-N	2.000	180.0
C2-H2-C2-N	2.000	180.0
C2-Zn-N-C1	2.000	180.0

VDW interaction			partial charges q (e)			
atom	ϵ (kcal/mol)	σ (Å)	Our Model	CBAC	REPEAT	DDEC
Zn	0.0125	1.960	+0.7362	+0.6970	-0.9807	+0.6920
N	0.1700	3.250	-0.3008	-0.4400	+0.4164	-0.3879
C1	0.0860	3.400	+0.4339	+0.6460	-0.1013	+0.4291
C2	0.0860	3.400	-0.1924	-0.0620	-0.3623	-0.0839
C3	0.1094	3.400	-0.6024	-0.0410	-0.7617	-0.4526
H2	0.0150	2.511	+0.1585	+0.0100	+0.2367	+0.1128
H3	0.0157	2.650	+0.1572	+0.0100	{+0.2463 +0.2792}	{+0.1325 +0.1306}

^a X denotes wildcard atoms: the given potential term is repeated for each possible dihedral combination X–A–B–X having A–B as central atoms.

^b Improper term A–B–C–D refers to the angle between planes A–B–C and B–C–D, with the B–C axis of rotation.

Here, we report a novel force field to perform molecular dynamics simulations in a flexible ZIF-8 system. This force field will be validated by testing its ability to reproduce correctly the ZIF-8 structure and by computing various dynamical properties of sorbed gas molecules to be compared with the literature results.

2. FRAMEWORK MODELING

2.1. Force Field Parameters. The framework interactions in our model can be divided in two parts, bonded and nonbonded. The bonded part consists in bond lengths and bond angles plus dihedrals and impropers angles. To model the organic linker we use the parameters taken from the AMBER²³ “parm10.dat” database, while the values of the parameters missing from the database are obtained via the “parmcal” calculator from the AmberTools suite (version 1.5). At the same time, ad-hoc parameters, optimized via quantum-chemical investigations,^{24–26} are used for the interactions of tetrahedral ZnN₄, due to their importance in describing the correct lattice behavior.^{4,20}

The nonbonded part, instead, consists of the van der Waals (VDW) forces modeled with Lennard-Jones parameters taken from AMBER and, in the electrostatic interactions, modeled using point charges placed on the framework atoms. The charges of our model have been computed in a previous paper using a series of *ab initio* calculations.²⁷

The functional form and the numerical values of all the relevant force field parameters are reported in Table 1, where the parameters for the interaction between atoms of different species, not shown, are obtained via usual Lorentz-Bertelot combining rules. In our parametrization, we neglect the torsion terms N–Zn–N–C1 and N–Zn–N–C2 (see inset figure in Table 1) to ensure a higher mobility of the MeIM organic linkers with respect to each other. At the same time, we allow a free rotation of the methyl group by setting to zero the torsion term N–C1–C3–H3, in accordance with the experimental measurement of Zhou and co-workers.²⁸

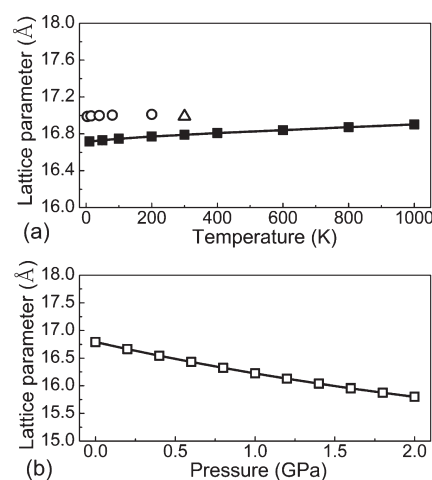
2.2. Force Field Validation. We start the validation of our force field focusing on the structural properties of the simulated ZIF-8 crystal. To do this, we perform molecular dynamics (MD)

Table 2. Comparison of Equilibrium Structural Parameters from our Model Framework with Experimental Data

average bond length		
type	expt ^a (Å)	simul (Å)
C1–C3	1.492	1.484
C1–N	1.339	1.330
C2–N	1.371	1.373
C2–C2	1.347	1.348
Zn–N	1.987	1.986
average bond angle		
type	expt ^a (deg)	simul (deg)
N–C1–N	112.2	111.8
N–C1–C3	123.9	124.0
C2–C2–N	108.7	108.0
C2–C2–H2	125.7	125.6
N–C2–H2	125.7	126.0
C1–C3–H3	109.5	109.6
C1–N–C2	105.2	105.8
C1–N–Zn	128.4	126.5
C2–N–Zn	126.4	127.3
N–Zn–N	109.8	109.4
average dihedral angle		
type	expt ^a (deg)	simul (deg)
C1–N–C2–C2	0.4	1.1
Zn–N–C2–C2	179.2	178.9
N–C2–C2–N	0.0	0.0
C3–C1–N–C2	176.9	178.8
C3–C1–N–Zn	1.8	2.0
N–C1–N–C2	0.7	1.1
N–C1–N–Zn	179.5	178.4
H2–C2–C2–H2	0.0	2.0
N–C2–C2–H2	180.0	180.0

^a Taken from Park and co-workers.¹

simulations in the isothermal–isobaric ensemble (*NPT*) at a fixed temperature of 300 K and pressure of 10^5 Pa, using the NAMD²⁹ package (version 2.8) with the barostat fluctuations controlled via Langevin piston Nosé–Hoover method. We set the piston oscillation period to 0.2 ps and the piston decay time to 0.1 ps. The damping coefficient for the temperature coupling is set to 10.0, giving a decay time of 0.1 ps. For all interactions (i.e., bonded, VDW, and electrostatic), a time step of 1.0 fs is used. The simulation box consists of $2 \times 2 \times 2$ unit cells (for a total of 2208 framework atoms), so that the VDW interaction cutoff (set to 14.0 Å) is smaller than half the box length, with cubic periodic boundary conditions (PBC) applied along the three main coordinate directions. Electrostatic interactions are treated via the particle mesh Ewald (PME) method. Note that, for each framework atom, a “scaled1–4” policy is applied; i.e., both the VDW and electrostatic interactions between couples of bonded atoms (1–2) or between atoms bonded to a common atom (1–3) are excluded, while for the interaction between atoms separated by two other atoms (1–4) the VDW “ ϵ parameter” for

**Figure 1.** Lattice parameters of ZIF-8 crystal structure over a wide range of (a) temperature and (b) pressure. Also in part a, available experimental data coming from X-ray diffraction⁶ (open triangle) and neutron powder diffraction²⁸ (open circles). Lines are to guide the eye.

the given couple is divided by 2 while the electrostatic interaction is divided by 1.2.

After equilibrating the system, we collect the trajectories of all the framework atoms for 1 ns and we compute the average bond length and bond angle values, finding that these are in good agreement with the data coming from X-ray diffraction experiments, see Table 2.

Then, using runs of 10 ns, we check the stability of our model framework over a wide range of temperature and pressure. As shown in Figure 1a, the thermal expansion trend is comparable with the experimental data.^{6,28} In particular, at 300 K and 10^5 Pa, the percentile difference between experimental⁶ (16.99 Å) and simulated (16.79 Å) lattice parameter is about 1% (in our simulation, the fluctuation of the lattice parameter is about 0.02 Å, corresponding to 0.1% of its mean value). In Figure 1b, instead, we can appreciate the excellent structural stability at various pressures of the modeled crystal, with a variation of the lattice value of less than 6% over the investigated pressure range. It should be noted that a weak point of many flexible framework force fields is the occurrence, during an *NPT* simulation, of lattice collapses or of unacceptable variations in the lattice parameter. This is not the case for our force field.

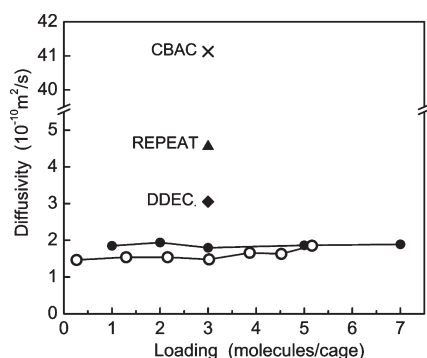
3. RESULTS AND DISCUSSION

3.1. CO₂ Self-Diffusivity. Before loading the sorbate into the crystal to perform self-diffusivity computations, we take the empty framework with its atoms initially located at their crystallographic position and run a 1 ns simulation in the canonical ensemble (*NVT*) to equilibrate the system at 300 K (via rescaling of the atoms velocities), followed by a 10 ns simulation in the microcanonical ensemble (*NVE*) to obtain the relaxed crystal structure (this operation is done only once for each set of framework parameters, i.e. only one relaxation for each charge model). The side length of each unit cell, forming the $2 \times 2 \times 2$ simulation box, is set to the experimental value⁶ of 16.99 Å (this choice is discussed in more detail in the Supporting Information). The simulation time step equals 1.0 fs.

Subsequently, we load the relaxed structure with the wanted number of CO₂ molecules and run a 1 ns *NVT* simulation to

Table 3. EPM2 Force Field Parameters for CO₂ Molecules³⁰

atom type	nonbonded interaction		
	ϵ (kcal/mol)	σ (Å)	q (e)
C	0.055 84	2.757	+0.6512
O	0.159 82	3.033	−0.3256

**Figure 2.** Comparison of self-diffusion coefficients for CO₂ in ZIF-8 for various charge models. From top of figure to bottom we find CBAC (cross), REPEAT (triangle), DDEC (diamond), and our charges²⁷ (circles); error bars are smaller than symbol size. Also shown is the experimental transport diffusivity from Bux et al.¹⁰ (empty circles).

equilibrate the system. At this point a 50 ns NVE production run is carried on. For the CO₂ interaction force field we use the EPM2 model of Harris and Yung,³⁰ see Table 3.

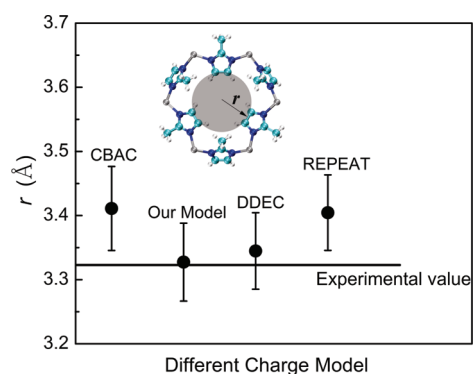
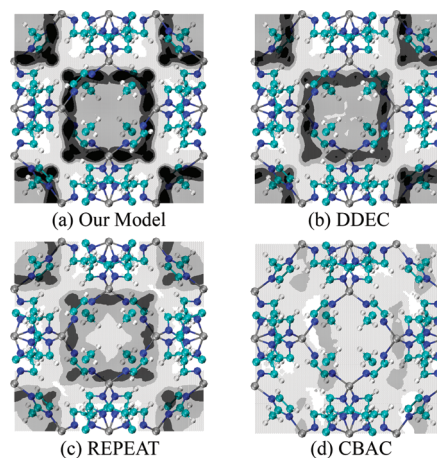
Figure 2 shows the self-diffusivities (D_S) values of CO₂ within flexible ZIF-8 computed by mean squared displacement (MSD) method using the Einstein relation:^{31–33}

$$D_S = \frac{1}{2d_0} \lim_{t \rightarrow \infty} \frac{d}{dt} \left\langle \frac{1}{N} \sum_{i=1}^N [\mathbf{r}_i(t) - \mathbf{r}_i(t_0)]^2 \right\rangle \quad (1)$$

where d_0 is the dimensionality of the system and $\mathbf{r}_i(t)$ is the position vector of sorbate molecule i at time t . In particular, the D_S value is averaged over all the N sorbed molecules and over multiple time origins t_0 (as symbolized by the brackets). These values are compared with available experimental values for the transport diffusion coefficients (D_T) derived from infrared microscopy (IRM).¹⁰ Note that, at low loadings, D_S and D_T should coincide.^{34,35} We can see that the D_S values coming from our charge model²⁷ show good agreement with IRM D_T . This result confirms the goodness of our point charges, in fact CO₂ is a polar molecule and, for this reason, it is sensitive to the electric field of the host lattice.

In Figure 2, we also present the CO₂ self-diffusivity computed at a loading of 3 molecules per cage (6 molecules/u.c.) using other charge models available in the literature,²² namely, the connectivity based atom contribution charge method (CBAC), the density derived electrostatic and chemical charge method (DDEC), and the repeating electrostatic potential extracted atomic charge method (REPEAT). We see that these charge models overestimate the self-diffusivity of CO₂ in comparison to the experimental results and to our model, in particular the discrepancy for the CBAC is of 1 order of magnitude.

These differences in self-diffusivity are explicable analyzing both: (1) the geometric properties and (2) the energetic properties

**Figure 3.** Average radius of 6-ring window in ZIF-8 computed for different charge models, to be compared with experimental values taken from XRD measurements.⁶**Figure 4.** Isoprobability contours for CO₂ inside one unit cell of ZIF-8, xy-plane projections computed for different charge models, with darker areas denoting higher probability.

of the system. On one hand, the point charges influence the equilibrium position of the framework atoms, which is responsible for the geometric factor (i.e., affecting the various sizes of the pore opening). On the other hand, they influence the interactions between the framework atoms and the sorbate molecules, which is responsible for the energetic landscape of the sorbate (i.e., the various locations of the sorption sites). Ultimately, the size of the window affects the cage to cage (intercages) mobility of the sorbate, while the location and the strength of the sorption sites affect both the mobility within each single cage (intracage) and the mobility between neighboring cages.

To study the first contribution, geometric factor, in Figure 3 we plot the size of the 6-ring window connecting two adjacent cages for the different charge models; we see that the window size coming from our force field is in good agreement with the experimental value,⁶ and it is sensibly smaller than the window size for the other charge models. To compute the window size (see inset of Figure 3), an ad-hoc routine has been developed. Given the position of the six carbon atoms forming the windows (labeled as C2 atoms in Table 1), our routine computes the mid point of each couple of carbon atoms and gives the radius of the sphere passing through these three points. The hydrogen atoms (labeled as H2 in Table 1 and bonded to the C2 atoms) have been

Table 4. Self-Diffusion Coefficients for CO₂ in ZIF-8, Computed for Different Systems and Their Ratio with Respect to the Reference Value

simulation models	D_s (10^{-10} m ² /s)	ratio
<i>uncharged-crystallographic</i>	10.46 ± 0.36	5.8
<i>charged-crystallographic</i>	3.87 ± 0.65	2.2
<i>charged-relaxed</i>	2.31 ± 0.33	1.3
<i>charged-flexible</i>	1.79 ± 0.10	1.0

neglected in the computation of the window size due to their higher mobility with respect to the C2 atoms. In Figure 3, the experimental result is obtained by applying our routine to the crystallographic position⁶ of the atoms.

The second contribution, energetic factor, can be evaluated looking at the isoprobability contours³⁶ for CO₂ inside ZIF-8 (Figure 4). We see that the density profile of the guest molecules is more homogeneous for the CBAC charge model than for the other charge models; in particular, our model²⁷ gives a strongly structured sorbate distribution function with the presence of well-defined sorption sites, which results in both intra- and inter-cage free energy barriers. To obtain the sorbate probability profile, we post process the sorbate trajectory by rescaling all the sorbate molecules coordinates to the primitive unit cell via ad hoc PBC. Then, discretizing the simulation box in cubic bins (each of side 0.34 Å), we compute the probability (p) to find a sorbate molecule in the given bin, satisfying the condition $\int_V P(x,y,z) dx dy dz = 1$ where V is the volume of the primitive unit cell. The isoprobability contours are plotted using the VMD software.³⁷

3.2. Importance of Various Modeling Details. At this point, we focus the attention on our force field and try to evaluate the influence of flexibility and point charges on the self-diffusivity of CO₂. To do this, we fix the loading to three molecules per cage and compare the diffusivity in our fully flexible and charged system (taken as a reference being our best estimate), with the diffusivity computed in three ad hoc rigid systems. In these systems we vary the structure of the framework, crystallographic or relaxed (where relaxed means averaged over a 10 ns run with the charged flexible framework), and the presence or not of charges:

- *uncharged-crystallographic*, this is the simplest model with the framework atoms located at their crystallographic position having no partial charges;
- *charged-crystallographic*, the framework atoms are located at their crystallographic position but they also have point charges, good to evaluate the direct influence of charges on the self-diffusivity due to the modification they induce on the sorbate free-energy landscape;
- *charged-relaxed*, framework atoms are located at the equilibrium position (averaged during a simulation with our charged flexible framework) having also partial charges, good to isolate, when compared to the *charged-crystallographic* system, the indirect effect of partial charges over self-diffusivity due to the modification they induce on the framework shape (especially window opening size) and good to appreciate, when compared to our reference *charged-flexible* system, the contribution of flexibility on self-diffusivity.

The systems are ordered according to an increasing number of modeling details, allowing direct evaluation of the contribution of every single detail on the final self-diffusion result, see Table 4. As expected, the *uncharged-crystallographic* system, being the less accurate, gives a gross value of self-diffusivity (almost 6 times

larger than our best estimate). This result is sensibly improved (reducing it to 2 times larger) by adding the partial charges, *charged-crystallographic* system. This fact alone underlines the importance of the charge values for a correct modeling of the dynamics of polar molecules such as CO₂ in ZIF-8. Comparing the diffusivity result in the *charged-crystallographic* system to the one in the *charged-relaxed* system we can appreciate the influence of framework shape, in particular window opening size, over the sorbate dynamics (the improvement in the accuracy on computed self-diffusivity is from 2.2 to 1.3). Finally, we compare the *charged-relaxed* system to the *flexible-charged* one to appreciate the contribution of the framework flexibility to the diffusivity value.

It is important to note how the increase in the level of modeling detail (introduction of partial charges, correct framework shape and flexibility³⁸) determines the improvement in the computed self-diffusivity value, which finally becomes comparable to the experimental result. In the case of CO₂, the flexibility of the framework decreases the value of self-diffusivity (increasing the accuracy of the model system); instead, for sorbates having a kinetic radius greater than the window size, we expect that the flexibility will increase the value of the computed self-diffusivity, being a key factor in allowing the motion of the sorbate between neighboring cages (this motion would be impossible in a fixed framework). This is the case, for example, with the diffusivity of methane.^{4,10}

4. CONCLUSIONS

In this work, a novel force field for molecular dynamics simulations of fully flexible ZIF-8 has been presented. The structure parameters of ZIF-8 computed with this force field (such as bond length and angle and window size) are in good agreement with experimental values. Besides, our force field reproduces correctly the thermal and pressure stability of ZIF-8 crystal structure. Reliable diffusivities of CO₂ were obtained with our fully flexible force field and our charge model.²⁷ These results have been compared to charge models available in the literature, explaining the discrepancies on the basis of point charge influence on the movement of guest CO₂ molecules via control of the window size and of the sorbate free energy landscape. Subsequently, we studied the weight that various simulation details, regarding the system modeling, have on the self-diffusivity, isolating the importance of charges, framework shape and framework flexibility on the accuracy of the final diffusivity result. After these investigations, we conclude that the force field presented in this paper is suitable to study the dynamic properties of sorbed CO₂ molecules within the flexible structure of ZIF-8. The diffusivity of other sorbates will be the subject of upcoming work, together with the characterization of the window opening mechanism and the application of coarse-graining techniques (cellular-automata) to the system dynamics.³⁹ The probability of our ZIF-8 force field to other ZIF structures (e.g., ZIF-3 and ZIF-90) will also be investigated in future studies.

■ ASSOCIATED CONTENT

S Supporting Information. Discussion regarding the influence of lattice parameter over the computed D_s value. This material is available free of charge via the Internet at <http://pubs.acs.org>.

■ AUTHOR INFORMATION

Corresponding Author

*Fax: +39 079 229559 E-mail: msant@uniss.it.

■ ACKNOWLEDGMENT

Support via India-European Union collaborative project AMCOS (233502) is kindly acknowledged. We thank Dr. M. Masia, Dr. F. G. Pazzona, and Dr. M. K. Rana for useful discussions.

■ REFERENCES

- (1) Park, K. S.; Ni, Z.; Côté, A. P.; Choi, J. Y.; Huang, R.; Uribe-Romo, F. J.; Chae, H. K.; O'Keeffe, M.; Yaghi, O. M. *Proc. Natl. Acad. Sci. U.S.A.* **2006**, *103*, 10186.
- (2) Li, J. R.; Ma, Y.; McCarthy, M. C.; Sculley, J.; Yu, J.; Jeong, H. K.; Balbuena, P. B.; Zhou, H. C. *Coord. Chem. Rev.* **2011**, *255*, 1791.
- (3) Banerjee, R.; Phan, A.; Wang, B.; Knobler, C.; Furukawa, H.; O'Keeffe, M.; Yaghi, O. M. *Science* **2008**, *319*, 939.
- (4) Hertäg, L.; Bux, H.; Caro, J.; Chmelik, C.; Remsungen, T.; Knauth, M.; Fritzsche, S. *J. Membr. Sci.* **2011**, *377*, 36.
- (5) Battisti, A.; Taioli, S.; Garberoglio, G. *Microporous Mesoporous Mater.* **2011**, *143*, 46.
- (6) Moggach, S. A.; Bennett, T. D.; Cheetham, A. K. *Angew. Chem., Int. Ed.* **2009**, *48*, 7087.
- (7) Fairen-Jimenez, D.; Moggach, S. A.; Wharmby, M. T.; Wright, P. A.; Parsons, S.; Düren, T. *J. Am. Chem. Soc.* **2011**, *133*, 8900.
- (8) Bux, H.; Feldhoff, A.; Cravillon, J.; Wiebcke, M.; Li, Y. S.; Caro, J. *Chem. Mater.* **2011**, *23*, 2262.
- (9) Bux, H.; Chmelik, C.; Krishna, R.; Caro, J. *J. Membr. Sci.* **2011**, *369*, 284.
- (10) Bux, H.; Chmelik, C.; Van Baten, J. M.; Krishna, R.; Caro, J. *Adv. Mater.* **2010**, *22*, 4741.
- (11) Gücüyener, C.; Van Den Bergh, J.; Gascon, J.; Kapteijn, F. *J. Am. Chem. Soc.* **2010**, *132*, 17704.
- (12) Venna, S. R.; Carreon, M. A. *J. Am. Chem. Soc.* **2010**, *132*, 76.
- (13) Sirjoosingh, A.; Alavi, S.; Woo, T. K. *J. Phys. Chem. C* **2010**, *114*, 2171.
- (14) Pantatosaki, E.; Pazzona, F. G.; Megariotis, G.; Papadopoulos, G. K. *J. Phys. Chem. B* **2010**, *114*, 2493.
- (15) Liu, B.; Smit, B. *J. Phys. Chem. C* **2010**, *114*, 8515.
- (16) Keskin, S. *J. Phys. Chem. C* **2010**, *115*, 800.
- (17) Guo, H. C.; Shi, F.; Ma, Z. F.; Liu, X. Q. *J. Phys. Chem. C* **2010**, *114*, 12158.
- (18) Zhou, M.; Wang, Q.; Zhang, L.; Liu, Y.-C.; Kang, Y. *J. Phys. Chem. B* **2009**, *113*, 11049.
- (19) Liu, D.; Zheng, C.; Yang, Q.; Zhong, C. *J. Phys. Chem. C* **2009**, *113*, 5004.
- (20) Salles, F.; Ghoufi, A.; Maurin, G.; Bell, R. G.; Mellot-Draznieks, C.; Férey, G. *Angew. Chem., Int. Ed.* **2008**, *47*, 8487.
- (21) Greathouse, J. A.; Allendorf, M. D. *J. Phys. Chem. C* **2008**, *112*, 5795.
- (22) Watanabe, T.; Manz, T. A.; Sholl, D. S. *J. Phys. Chem. C* **2011**, *115*, 4824.
- (23) Duan, Y.; Wu, C.; Chowdhury, S.; Lee, M. C.; Xiong, G.; Zhang, W.; Yang, R.; Cieplak, P.; Luo, R.; Lee, T.; et al. *J. Comput. Chem.* **2003**, *24*, 1999.
- (24) Peters, M. B.; Yang, Y.; Wang, B.; Füsti-Molnár, L.; Weaver, M. N.; Merz, K. M. *J. Chem. Theory Comput.* **2010**, *6*, 2935.
- (25) Lin, F.; Wang, R. *J. Chem. Theory Comput.* **2010**, *6*, 1852.
- (26) Hoops, S. C.; Anderson, K. W.; Merz, K. M., Jr. *J. Am. Chem. Soc.* **1991**, *113*, 8262.
- (27) Rana, M. K.; Pazzona, F. G.; Suffritti, G. B.; Demontis, P.; Masia, M. *J. Chem. Theory Comput.* **2011**, *7*, 1575.
- (28) Zhou, W.; Wu, H.; Udovic, T. J.; Rush, J. J.; Yildirim, T. *J. Phys. Chem. A* **2008**, *112*, 12602.
- (29) Phillips, J. C.; Braun, R.; Wang, W.; Gumbart, J.; Tajkhorshid, E.; Villa, E.; Chipot, C.; Skeel, R. D.; Kalé, L.; Schulten, K. *J. Comput. Chem.* **2005**, *26*, 1781.
- (30) Harris, J. G.; Yung, K. H. *J. Phys. Chem.* **1995**, *99*, 12021.
- (31) Allen, M.; Tildesley, D. *Computer Simulation of Liquids*; Oxford University Press: New York, 1987.
- (32) Einstein, A. *Ann. Phys.* **1905**, *17*, 549.
- (33) Chitra, R.; Yashonath, S. *J. Phys. Chem. B* **1997**, *101*, 5437.
- (34) Sant, M.; Leyssale, J.-M.; Papadopoulos, G. K.; Theodorou, D. N. *J. Phys. Chem. B* **2009**, *113*, 13761.
- (35) Papadopoulos, G. K.; Jobic, H.; Theodorou, D. N. *J. Phys. Chem. B* **2004**, *108*, 12748.
- (36) Sant, M.; Papadopoulos, G. K.; Theodorou, D. N. *J. Chem. Phys.* **2010**, *132*, 134108.
- (37) Humphrey, W.; Dalke, A.; Schulten, K. *J. Mol. Graphics* **1996**, *14*, 33.
- (38) Demontis, P.; Suffritti, G. B. *Microporous Mesoporous Mater.* **2009**, *125*, 160.
- (39) Pazzona, F. G.; Demontis, P.; Suffritti, G. B. *J. Chem. Phys.* **2009**, *131*, 234703.